

Experimental Investigations of Alkaline Silver-zinc and Copper-zinc Batteries

A. Habekost*

Department of Chemistry, University of Education, Reuteallee 46, D-71634 Ludwigsburg, Germany

*Corresponding author: a.habekost@t-online.de

Abstract Batteries are important issues in electrochemistry and in electrochemistry lessons. But nevertheless, the electrode processes in batteries are not quite easy to understand. One of the didactic benefits of the investigations of alkaline silver-zinc and copper-zinc batteries might be the chance to directly observe the changes on the electrode surface and the simple way to measure the electrode processes. These electrode processes are intensively examined so that they can be explained well and described clearly. In this paper we will present several experiments to investigate these two battery systems: Cyclic voltammetry is used to identify the electrode processes, and on the basis of charging and discharging curves one can estimate the efficiency of the batteries. Furthermore, the reflection of a laser beam onto a surface is an easy means to correlate the results with the electrochemical changes of the electrode.

Keywords: *Third-Year Undergraduate, analytical, electrochemistry, batteries, Hands-on Learning/Manipulatives*

Cite This Article: A. Habekost, "Experimental Investigations of Alkaline Silver-zinc and Copper-zinc Batteries." *World Journal of Chemical Education*, vol. 4, no. 1 (2016): 4-12. doi: 10.12691/wjce-4-1-2.

1. Introduction

Electrochemical power sources convert chemical energy to electrical energy. At least two redox couples undergo a chemical reaction during this operation. The existing types of battery systems vary according to the nature of the chemical reaction and the design of the battery. Primary cells are not rechargeable, and the chemical reaction is irreversible. Secondary cells are reversible, and this type is chargeable and dischargeable. The processes can be performed for hundreds or even thousands of times so that the lifetime of these cells can be several years [1].

A good battery shows a high cyclic stability. This means that such a battery's electrochemical behavior is stable with each charging and discharging process [1]. Moreover, the efficiency and the charge in the charging and discharging processes can be easily measured in the lab.

In chemistry teaching there are some electrochemical systems as well as primary and secondary cells. In particular, this includes the Daniell and Leclanche battery as primary cells, and NiCd- and Ni-Metalhydride as secondary cells. Recently, the Li-ion battery has become increasingly important in the fields of technological development and chemical education [2,3,4,5].

In this paper we present two other electrochemical systems having some important advantages in a didactical sense in comparison with the above-mentioned batteries. The electrode processes in the Ag-Zn battery in an alkaline solution can be monitored with the cyclic voltammetry method [6,7] and by the reflection of a laser beam onto a silver-electrode surface. In contrast to the

Daniell battery, the Cu-Zn battery in an alkaline solution shows different behaviors that are well understood [8]. Therefore, this type can be a significant extension in teaching electrochemistry.

2. The Silver-zinc Battery

Literature data in the database SciFinder [9] have resulted in 235 articles, including the keyword "silver zinc battery" (1952-2015). In the last few years the main investigations have been performed on the miniaturization of batteries and the improvement of the electrode materials by using nanomaterials to enhance the long-term stability [10].

In the period between the 1960s and the 1980s the electrochemical processes on the silver surface were especially investigated: With cyclic voltammetry [6,7], Stonehard and Portante [11] measured the electrochemical reaction on a silver electrode in a 1 M NaOH solution. On the basis of chronoamperometric measurements [12] they calculated the kinetics of the AgO-formation. At first, AgO was formed at a positive potential, and the decrease of AgO was measured as a function of time at a negative potential. The formation of AgO and Ag₂O was observed by variation of the oxidation potential.

Pound et al. [13,14] investigated the electrochemical processes on polycrystalline silver at different temperatures between 295 K and 478 K in a 1 M KOH solution; they calculated the temperature-dependent charge-capacity of a silver-electrode. Hence, they could show that the surface-processes are diffusion-controlled. It means that the electron-transfer reaction was faster than the diffusion of OH⁻ to or from the electrode.

Transient current measurements as a function of potential and temperature show that the formation of AgO and Ag₂O starts at a specific threshold potential [13,14].

Lazarescu et al. [15] measured the processes on a silver surface in an alkaline solution in the presence of chloride ions. Giles and Harrison [16] compared the results of the electrochemical behavior of silver single crystals and polycrystalline silver.

2.1. Experimental Procedure

2.1.1. CV of Ag in KOH

One of the most important experimental methods to investigate redox systems for being used as rechargeable batteries is cyclic voltammetry. Therefore, this paper initially presents and interprets the cyclic voltammograms of the Ag-Zn system in an alkaline solution.

Chemicals and instruments:

Silver sheet (Hedinger, Germany, 834 AG), silver wire (Hedinger, Germany, 5199), zinc rod (Hedinger, Germany, 5190), Ag/AgCl/KCl (1 mol/L) (Phywe, Germany, 1875-00), KOH solution (20%), Potentiostat μ -Stat 400 (Dropsens).

Procedure: Place the electrodes in a 250 mL glass bottle with the electrolyte, and connect the electrodes in the following way: Connect the silver sheet as working electrode (WE), the silver wire as the counter electrode (CE), and the Ag/AgCl/KCl (sat.) as the reference electrode (RE, $E_{ref} \approx 0.22$ V) with the potentiostat.

Figure 1 shows the CV of a silver sheet in a KOH solution (20%) at a scan rate of 10 mV/s. Start potential -0.3 V, reverse potential 0.75 V, final potential -0.3 V.

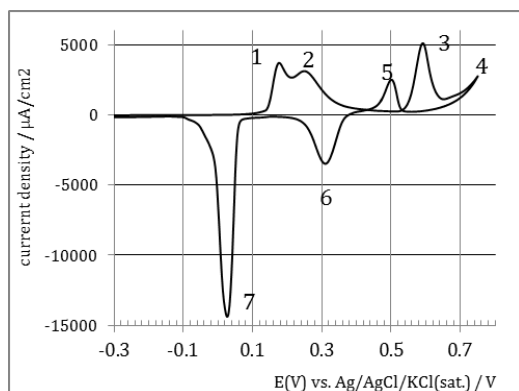
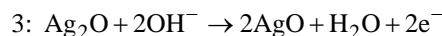
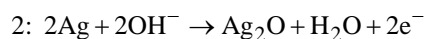


Figure 1. CV of a silver sheet in a 1mol/L KOH solution. Scan rate 10 mV/s. Peak 5 is formed in the reverse voltage run (see the numerical sequence)

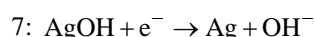
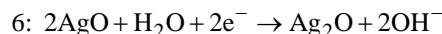
The CV shows four oxidation peaks (positive current peaks 1, 2, 3, and 5), and two reduction peaks (negative current peaks 6 and 7). The increase in the current of peak 4 results in the beginning of the formation of oxygen from decomposition of the alkaline water according to the oxidation $4\text{OH}^- \rightarrow \text{O}_2 + 2\text{H}_2\text{O} + 4\text{e}^-$.

Up to a voltage of about 0.1 V the silver surface does not react (see also Figure 2a). Afterwards, it forms brown Ag(OH) and Ag₂O (Peaks 1 and 2, see also Figure 2b), and then black AgO (Peak 3, see also Figs. 2 d and e):



By reversing the voltage, the silver electrode becomes brighter at 0.3 V (peak 6), and is almost silver-colored beginning at 0 V (peak 7).

One can calculate the standard potential E_0 ($=1/2(E_{\text{Oxidation}} + E_{\text{Reduction}})$) for the redox couples which are represented by the peaks 1-2 / 7 and 3 / 6 (see [17]).



The current peaks of the anodic and cathodic peaks differ about 250 mV or 130 mV. This means that the corresponding reactions are quasi-reversible [6,7] (a reversible one-electron process causes a potential difference between oxidation and reduction peak of 59 mV), and diffusion and electron transfer reaction are within the same time-scale.

Table 1. Summary of the measured peak potentials in comparison to those of reference [11]

Redox couples	Standard Peak potential (peak potential after [11]) / V	Electrode reaction
1 / 7	0.40 (0.39)	$\text{Ag} + \text{OH}^- \leftrightarrow \text{AgOH} + \text{e}^-$
2 / 7	0.46 (0.47)	$2 \text{Ag} + 2 \text{OH}^- \leftrightarrow \text{Ag}_2\text{O} + \text{H}_2\text{O} + 2\text{e}^-$
3 / 6	0.80 (0.80)	$\text{Ag}_2\text{O} + 2\text{OH}^- \leftrightarrow 2\text{AgO} + \text{H}_2\text{O} + 2\text{e}^-$

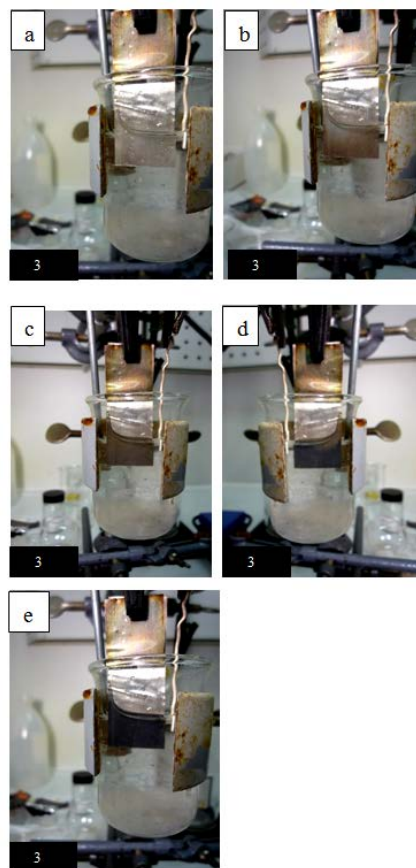


Figure 2. Silver electrode at different potentials: a) 0.3 V to 0.11 V: Ag, b) approximately 0.2 V: Ag₂O, c): approximately 0.4 V: Ag₂O, d) 0.6 V: Ag₂O and "AgO," and e) 0.65 V: "AgO."

The oxidation peak 5 is somewhat surprising because the oxidation occurs after reducing the potential. In [11] this phenomenon is explained by the completion of the AgO surface and described as “secondary AgO”. That means that the surface forms AgO multilayers.



Formation of AgO is non-stoichiometric [11]. This is the result of the measured charge responsible for the formation of AgO from Ag₂O and of Ag₂O from Ag, because the charge of the formation of AgO from Ag₂O was not equivalent to the charge for the formation of Ag₂O from silver. If one assumes that the silver atoms within the reaction layer are equally accessible for oxidation and that the oxidation and reduction characteristics of the silver oxides are completely reproducible, AgO must be nonstoichiometric.

It is also known that the AgO species is neither simple AgO nor Ag₂O₂ because AgO might be paramagnetic and Ag₂O₂ might form H₂O₂ by acidification, but this does not occur. Instead, AgO is the mixed oxide Ag^IAg^{III}O₂, where each Ag⁺ is linearly surrounded by two O-atoms and each Ag³⁺ square surrounded by four O-atoms [23].

In [24,25,26] it was shown that x-ray diffraction and magnetic measurements suggest that approximately every 6th Ag-atom in AgO is an Ag^{III} species. Later, we will return to this point.

2.1.2. Charging and discharging curves

The charging and discharging curves of silver was published in 1908 for the first time [27]. We will follow this historical experiment.

Chemicals and instruments:

Silver sheet (Hedinger, 834 AG), Zinc rod (Hedinger, 5190), KOH-solution (20%), Sensor Cassy (LD-Didactic), Power Cassy (LD-Didactic), Charging and discharging resistor (10-coil potentiometer: max. 100 Ohm)

Procedure: Connect the silver sheet and the zinc rod in the KOH solution with the Power Cassy power supply, the charging / discharging resistor, and the Sensor Cassy which acts as a voltmeter: the charging curve.

For the recording of the discharge curve one has to switch a relay (this can be done by Sensor Cassy), and disconnect the power supply.

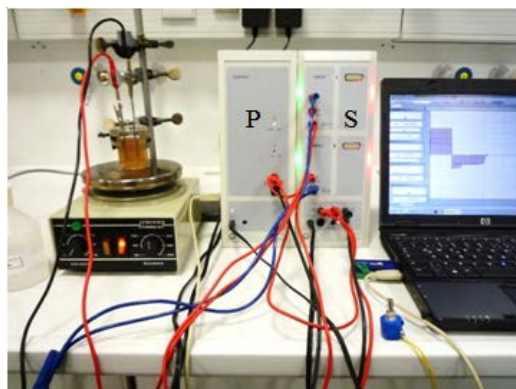


Figure 3. Experimental equipment for detecting charging and discharging cycles. On the left: the Ag-Zn battery in a beaker on a stirrer. In the middle: power supply (Power Cassy, P) with data acquisition (Sensor Cassy, S). On the bottom left from the notebook: charging and discharging potentiometer (blue). The relay switches between charging and discharging process

The potential and time were recorded by the data acquisition system Sensor Cassy. After each charging time (50 s with a charging potential of 7 V) over a load resistance of 120 Ohm, an electronic relay is switched and the discharging is recorded over 150 s.

After 200 s, the charging cycle starts again. Charging can be performed either by a rectangular pulse (7 V for 50 s) or by a voltage ramp (0 V linear to 7 V in 50 s, freely programmable).

Figure 4 shows twenty charging and discharging cycles. As the curves only differ slightly, the cyclic stability is within the scope of the measurement accuracy.

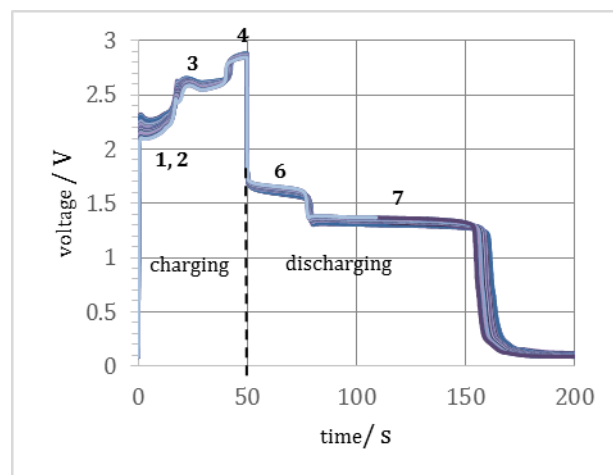
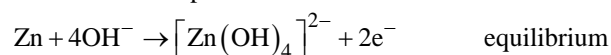


Figure 4. Twenty cycles of charging and discharging. Charging time: 50 s (voltage ramp 0 → 7 V) followed by discharging. The numbers correspond to the current peaks in Figure 1 and the reaction equations, respectively

The potential-values between CV and the curves of Figure 4 differ because in CV the potential of the WE refers to the electrochemical reference, whereas in the measurement of Figure 4 it refers to the potential of the Zn/Zn²⁺ in alkaline potential:



$$-1.215 \text{ V [15]} \quad (1)$$

Thus, one can calculate the following EMF (electromotive force)-values:

$$6: \text{EMF}_6(2\text{AgO} / \text{Ag}_2\text{O} // \text{Zn} / \text{Zn}^{2+}) = 0.6 \text{ V} - (-1.215 \text{ V}) \approx 1.8 \text{ V} \quad (2)$$

$$7: \text{EMF}_7(2 \text{Ag}_2\text{O} / \text{Ag} // \text{Zn} / \text{Zn}^{2+}) = 0.345 \text{ V} - (-1.215 \text{ V}) \approx 1.56 \text{ V} \quad (3)$$

A comparison between the experimental and theoretical values (EMF₆ ≈ 1.7 V and EMF₇ ≈ 1.4 V) shows only little difference (one has to consider that the measured voltage is not the open-circuit voltage because a current of about 20 mA flows. But the internal resistance of the voltmeter is much higher than the internal resistance of the battery and therefore the deviation is low).

Following Dierkse [24,25,26] Allen [23] describes the peak between Ag₂O and AgO (in Figure 4, peak 3): this peak is produced by a concentration of current into small

localized areas where the conversion of Ag_2O to AgO can proceed. This causes an increased overvoltage for the conversion reaction.

In a simply way, one can calculate the efficiency η , defined by $\eta = E_{\text{discharging}} / E_{\text{charging}}$, and the charge flowing by charging and discharging process $Q = \int I dt$ (Figure 5 and Figure 6).

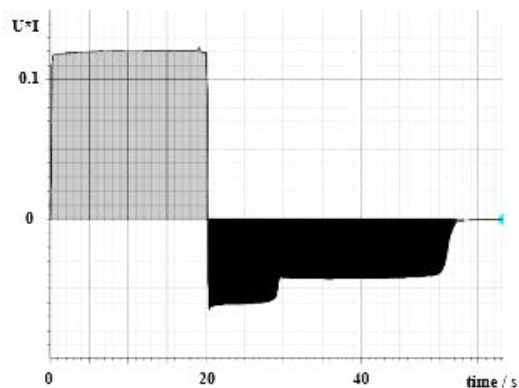


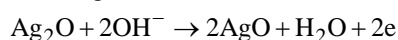
Figure 5. Calculation of the efficiency of the Ag-Zn battery by plotting the power $U \cdot I$ (the integral is the energy) vs t . Bright area: charging energy (2.4 J). Dark area: discharging energy (1.5 J)

We can calculate the efficiency of the Ag-Zn battery by

$$\eta = (\int U \cdot I dt)_{\text{discharging}} / (\int U \cdot I dt)_{\text{charging}}$$

This results in $\eta = 1.5\text{J} / 2.4\text{J} = 62\%$ - quite a reasonable result [28].

The charge Q characterizes the oxidized quantity of substances (e.g. Ag_2O) formed on the silver surface (in the elementary step the formation of Ag_2O required two electrons according to the reaction $2\text{Ag} + 2\text{OH}^- \rightarrow \text{Ag}_2\text{O} + \text{H}_2\text{O} + 2e^-$), which subsequently reacts to AgO :



and vice versa.

For calculating the charge flowing out of the battery, one has to measure the current vs time (Figure 6). First, the battery was charged (loading resistor: 50 Ohm). After 20 s, the battery was discharged via the same resistor.

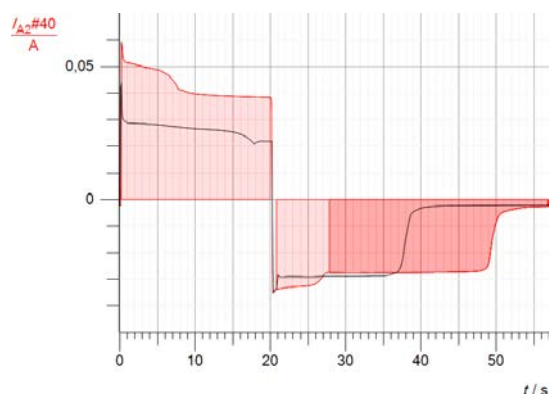


Figure 6. Current I is plotted vs time t for two different charging voltages (charging time 20 s, respectively). The upper, left area (bright red area) is the total charge for the charging reaction (0.84 A·s), while the lower right area is the charge for the discharge reaction (0.82 A·s). In addition, the latter area is divided into the charge which results in the reaction $\text{AgO} \rightarrow \text{Ag}_2\text{O}$ (bright, lower area: 0.2 A·s) and the charge from reaction $\text{Ag}_2\text{O} \rightarrow \text{Ag}$ (dark, lower area: 0.62 A·s)

The discharge curve (starting from 20 s) shows the two involved redox systems, but only if the charging voltage exceeds the voltage which is necessary to form AgO (red curve: $\text{AgO} \rightarrow \text{Ag}_2\text{O}$ and $\text{Ag}_2\text{O} \rightarrow \text{Ag}$). In case of a lower charging voltage, only the reaction $\text{Ag}_2\text{O} \rightarrow \text{Ag}$ occurs (black curve).

The total discharging charge is 0.82 A·s (lower, dark area in Figure 6) or 0.22 mA·h. This value is much lower than those of commercial batteries, which are more than a thousand times. This is because the electrode surface area is much smaller than the commercial ones (in our experiments: 9 cm^2 for the silver and 2 cm^2 for the zinc electrode).

It is also striking that the charge for the reduction of AgO to form Ag_2O is only about one-third of the total charge. As mentioned above, “ AgO ” consists of the non-stoichiometric chemical compound $\text{Ag}^I\text{Ag}^{III}\text{O}_2$, where Ag^{III} has a share of 1/6 in relation to Ag^I . Furthermore, since the reduction of Ag^{III} to form Ag^I needs two electrons, one can explain the charging relation of 1:3, which was confirmed by the experimental results above:

$$0.2\text{As} = 0.62\text{As} \approx 1:3.$$

2.1.3. Reflections on the silver surface

Chemicals and instruments:

Silver sheet (Hedinger, 834 AG), Zinc rod (Hedinger, 5190), KOH-solution (20%), Sensor Cassy (LD-Didactic), Power Cassy (LD-Didactic), Light sensor (LD-Didactic, 666243), Laser pointer (z.B. Hama LP-18), Quartz cuvette (Suprasil, Perkin-Elmer), Load resistor: 120 Ohm.

Procedure: Build up the experiment shown in Figure 7.

Figure 7 shows the experimental setup, and Figure 8 shows the results of the reflection of a laser beam onto a silver surface during the charging and discharging processes.

In Figure 8 one can see a marked correlation between the reflection intensity (black curve), and the charging and discharging voltage (red curve): from 30 to 85 s the light intensity decreases, as the silver surface first becomes brown (formation of Ag_2O). Afterward, the surface darkens ($\text{Ag}^I\text{Ag}^{III}\text{O}_2$).

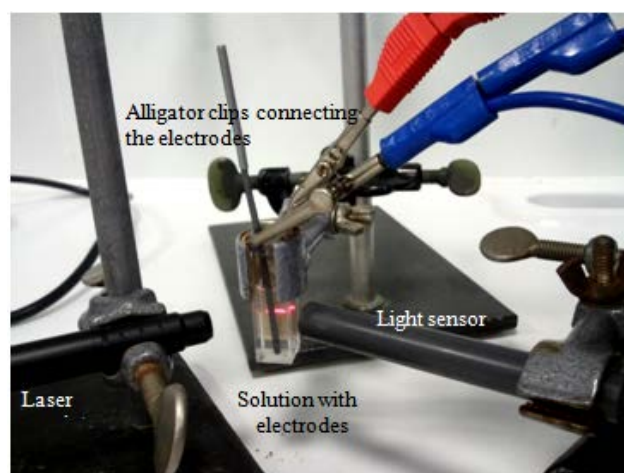


Figure 7. Photo of the experimental setup: simultaneously recording voltage and reflection. The beam of the laser pointer impinges the surface in an angle of 45°

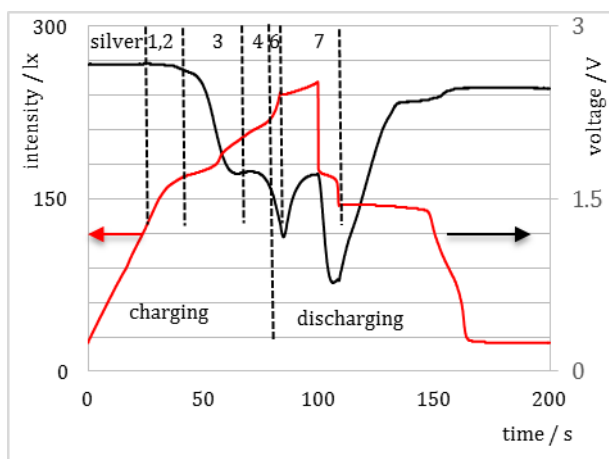


Figure 8. Results of the reflection intensity (black), and charging and discharging voltage (red). The numbers correlate with those of Figure 1 and the electrode reactions mentioned above. Charging-time: 100 s

After 85 s gas bubbles (oxygen, see 2.1.1) arise on the surface, the light intensity increases. After 100 s (see the dividing line between 4 and 6 in Figure 8), the charging stops and the reverse reactions occur. The gas bubbling now stops immediately, the black surface dominates the reflection. After 108 s the surface gets brighter (at first brown), and the initial silver-color returns at the end of the cycle.

3. The alkaline copper-zinc-battery

3.1. Background

The Daniell-battery in which copper and zinc are separately immersed in a solution of copper- and zinc salt is a typical electrochemical system / setup in teaching chemistry and in chemistry textbooks. The application of the Nernst equation, the calculation of the EMF as a function of concentration and temperature, and the comparison between theoretical and experimental values are the main topics. For students, in particular, the precise meaning of the electrode potential is difficult to understand and often a cause of students' (and teachers') misconceptions.

In addition, the passivity of copper is interesting with regard to basic and applied research due to its wide application in industry (keywords being metallic conductors and corrosion). Thus, electrochemical (and spectroscopic) quantities provide information about the behavior of copper in different media.

In 1894 Schoop [29] elaborated that in trans the alkaline copper-zinc battery is a serious alternative to the lead battery.

Since that time there exists a plethora of different investigations of the electrochemical behavior of copper. Our paper lists only a few of the results.

In the 1970s Leckie [30] studied the oxidation of Cu in both acidic and alkaline media. Ambrose [31] investigated the copper electrode as well, and explained the different anodic and cathodic current peaks. Dong [32] combined cyclic voltammetry with spectro-electrochemical studies. They deposited Cu on a tin oxide / glass surface in a potassium hydroxide electrolyte and measured in situ the transmission of the surface. They found that this system

has the same CV as pure copper, but the electrode affords a much more resolution.

El Haleem [33] measured the CV of the copper electrode in NaOH solution as a function of scan rate, electrolyte concentration, and potential range. They pointed out that the main anodic peaks are the formation of a monolayer of Cu_2O followed by the formation of a thick multilayer film of CuO. They concluded that the CuO was formed both from direct oxidation of copper metal and from oxidation of Cu_2O . They summarized that the behavior of the copper metal in alkaline solution is quite complicated because there is not a simple relation between the scan rate and the current peaks, as suggested by the equation of Randles-Sevcik [6,7]. Lorimer et al. [8] investigated the passivation phenomenon of copper during ultrasonic irradiation. They found that irradiation can significantly promote the anodic oxidation of copper, which leads to a thicker and more porous copper oxide / hydroxide layer. The application of ultrasound activates the Cu-surface and increases the peak currents.

Strehblow et al. [34] combined cyclic voltammetry with scanning tunnel microscopy (STM) measurements (so-called "electrochemical STM") and published several STM images of the development of OH adsorption on Cu and of the growth of Cu_2O at different potentials. Based on a band model of Cu, they explained the redox processes and the band deflection for increasing potentials and for passivating Cu_2O on Cu. The explanations also took the electron transfers in an alkaline solution into account.

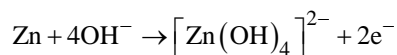
It was the intention of Baricuatro [35] to investigate whether Cu is a good catalyst for the reduction of carbon dioxide. However, it is an established fact that Cu is an excellent scavenger of oxygen. Electrochemical and surface-analytical methods such as LEED (low energy electron diffraction) and Auger spectroscopy under UHV (ultrahigh vacuum) conditions show a different behavior of different single-crystal copper electrodes - e.g. Cu (110), Cu (100) and Cu (111).

The temperature dependence of the formation of Cu_2O islands on Cu (110) [36] and Cu (001) [37] was investigated by Zhou and Yang with UHV-transmission electron microscopy (UHV-TEM). They found an epitaxial, i.e., oriented three-dimensional growth of Cu_2O on Cu. They also examined the oxidation kinetics of a Cu (110) film with UHV-TEM [38] and found a nucleation of the oxide islands as a function of time after an incubation period of several minutes. After about 20 minutes, the islands reach a saturation intensity of the nuclei.

3.2. Experiments and Results

We think that the investigation of the copper-zinc battery (just like the Ag-Zn battery) fulfills the didactic criteria of clearness and self-activeness because the electrode reactions are exactly identified, and all relevant physicochemical parameters such as charge, efficiency, and open-circuit voltage can easily be investigated with this kind of batteries.

First, we investigated the Cu-electrode processes with cyclic voltammetry. The zinc-electrode reaction in an alkaline electrolyte is the same as in the Ag-Zn battery a simple formation of a zinc-hydroxide complex:



Chemicals and instruments:

Copper sheet (Hedinger), zinc rod (Hedinger, 5190), Na_2CO_3 -solution (different concentrations), copper sulfate solution ($c = 0.001 \text{ mol/L}$), membrane from a Li^+ -battery, potentiostat $\mu\text{-Stat 400}$ (Dropsens).

Procedure: Build up the experiment analogous to that described in 2.1.1.

Figure 9 shows the CV of Cu in different sodium carbonate solutions (different pH values)

The CV was recorded in the following way: start potential -0.9 V , reversed potential 0.6 V , final potential -0.9 V , scan rate 20 mV/s (here we used this scan rate to better identify the current peaks), Cu as WE, Ag/AgCl/KCl (3 mol/L) as RE, and Zn rod as CE. The arrow in Figure 9 indicates the increasing pH (11, 11.5, 12, 12.5, 13). The increase of the current peaks as a function of the increasing pH corresponds to the equation of Randles-Sevcik, in which the current is proportional to the concentration of the electroactive species. This means that the solubility of copper must be much better in alkaline solutions than in water.

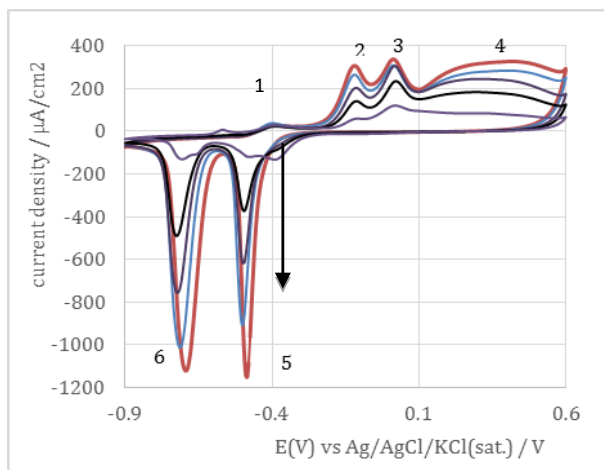
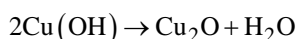
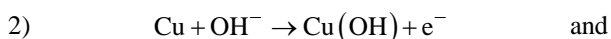
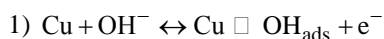
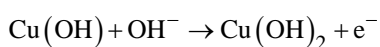
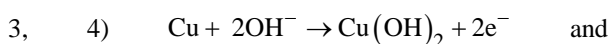


Figure 9. CV of Cu in alkaline solutions at different pH (11-13). Scan rate 20 mV/s (then arrow indicates increasing pH). After each run the electrode was intensively rinsed with water

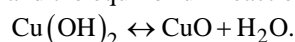
El Haalem [30] and Streblov [34] label the following peaks (see also Figure 9):



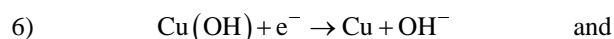
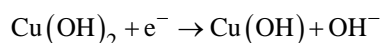
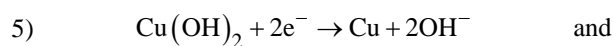
El Haalem emphasized that one can see no tarnishing of the metal surface. So, it is possible that only a monolayer gets formed.



and the equilibrium reaction



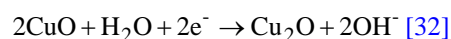
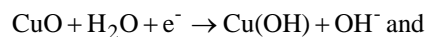
In addition, Cu_2O can produce CuO and also Cu in a direct, two-electron process. El Haalem suggested that the major portion of the resulting CuO is obtained directly from Cu via a two-electron transfer reaction.



Compared to the other peaks peak 4 is remarkable broad. Lorimer et al [8] interpret this phenomenon as formation of a layer containing cuprous oxide and cupric oxide/hydroxide with a duplex structure, i.e. $\text{Cu/Cu}_2\text{O/CuO}$, $\text{Cu}(\text{OH})_2$. They showed that the passive layer has an inner Cu_2O part and an outer $\text{CuO/Cu}(\text{OH})_2$ part which leads to a broadening of the current peak. El Haalem emphasized that the broad peak is the result of the formation of CuO multilayers

The potential of the current peaks differ significantly as a function of pH to more negative values. This is consistent with the Pourbaix diagram of copper [39].

Figure 10 shows the CV for a Cu electrode, which was produced in situ from a diluted copper sulfate solution ($c = 0.001 \text{ mol/L}$). The thin copper surface affects the splitting of one of the reduction peaks. This phenomenon can be explained by the two reactions:



Only in a diluted solution this splitting can be observed as Figure 10 indicates.

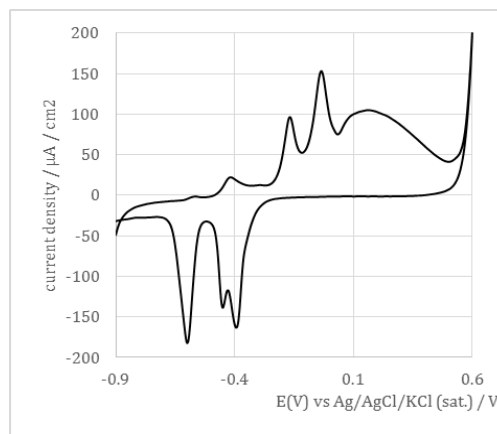


Figure 10. CV of in situ produced Cu of a solution of CuSO_4 . The diluted copper salt solution ensures that the copper layer is quite thin. CV after intense rinsing the electrode in an alkaline solution

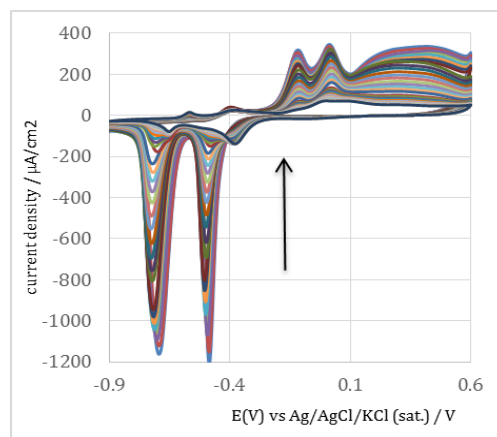


Figure 11. CV of Cu in alkaline solution 20 times: gradual decrease of all current peaks (see arrow). Scan rate 20 mV/s

All current peaks decrease if one records the CV several times (Figure 11). We suggest that the copper electrode is coated with a copper oxide or hydroxide layer. This layer can be removed after intense rinsing the electrode.

In the following CV we examined the anodic and cathodic peak at -0.56 V and -0.66 V more precisely. As mentioned above, Strehblow et al. [34] identified these peaks as OH adsorption and desorption according to the reaction



Figure 12 shows a shift of the peak potentials for increasing scan rates. This means that the process is quasi-reversible, the diffusion of OH^- and the electron-transfer reaction are on the same time scale. The measured charge-density for both peaks is about $100 \mu\text{C}/\text{cm}^2$. This corresponds to a surface concentration of $6 \cdot 10^{14} \text{ cm}^{-2}$. With an assumed diameter of Cu of $1.28 \cdot 10^{-8} \text{ cm}$, a 1 cm^2 surface comprises $7 \cdot 10^{15}$ Cu-atoms. It means that the measured charge is formed by one tenth of a multilayer.

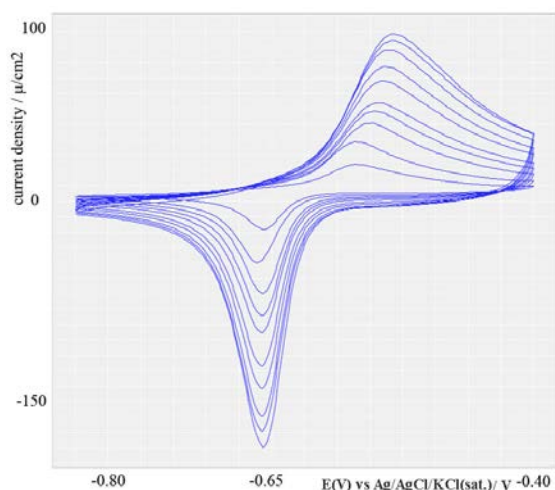


Figure 12. Scan rate dependence of the CV of Cu in a sat. Na_2CO_3 solution in the range between -0.8 V and -0.45 V

The following Figure 13 shows the copper and the zinc sheets before and after over a hundred charging / discharging cycles. It is obvious that the copper surface darkens (formation of CuO) and the zinc surface gets frayed (dissolving of zinc). As a membrane between copper and zinc, we use a polymer from the Li-ion battery. These are often microporous materials - e.g. polyethylene (PE) or polypropylene (PP). Both materials have excellent mechanical and chemical characteristics. Sometimes a laminate of PP/PE/PP is used, too [1].

Figure 14 shows the experimental setup for charging and discharging of the Cu-Zn battery: the sandwich Cu-Zn battery is inside the beaker with the electrolyte, the electrolyte was stirred.

The recording of the charging and discharging cycles occurs in the same manner and with the same materials as described above for the Ag-Zn battery. In Figure 15 we show the voltage and current curve for charging and discharging with different resistors.

Chemicals and instruments:

Copper sheet (Hedinger, 834 AG), Zinc rod (Hedinger, 5190), Sodium carbonate solution (sat.), Sensor Cassy (LD-Didactic), Power Cassy (LD-Didactic), Small-current

motor, Charging and discharging resistors (120 Ohm , 1000 Ohm).

Procedure: Analogous to the experiment described in 2.1.2.



Figure 13. Photos of the used copper and zinc sheet. Top: before, bottom: after use as electrodes in the Cu-Zn battery. On top: white: the separators. The materials were wound as a sandwich: Cu - separator - Zn - separator. Metal loops at the end of the two metals were connected with alligator clips

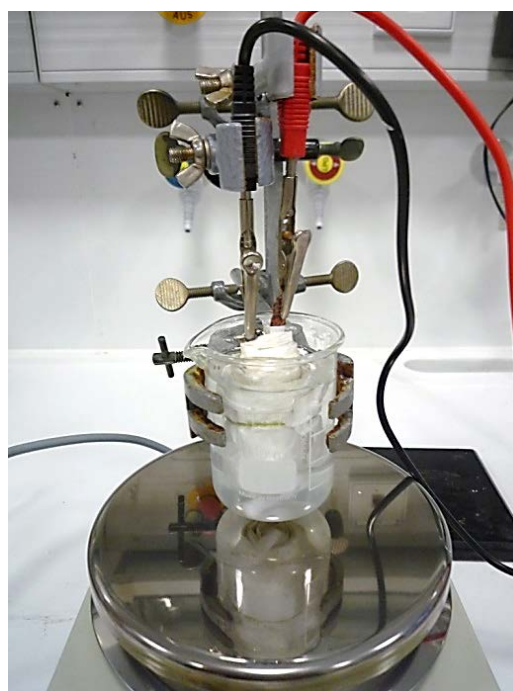


Figure 14. Cu-Zn battery inside the beaker with the stirred electrolyte (sodium carbonate)

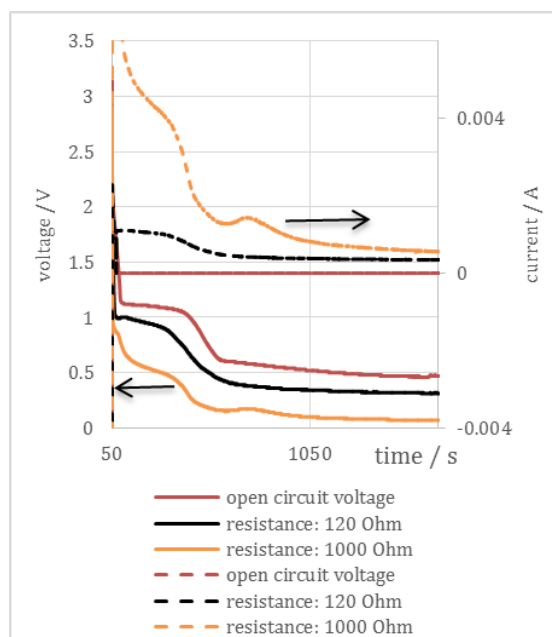


Figure 15. Voltage and current as a function of time and charging / discharging resistors. Solid lines: voltage, dotted lines: current

After charging (50 s), the open-circuit voltage is about 1.1 V, and then the voltage decreases to about 0.5 V. This value is stable for more than 1000 s.

If we use a charge / discharge resistor of 1000 Ohm and 120 Ohm, the voltage decreases more rapidly but at different speeds. With this simple setup one can operate a small-current motor (resistance about 200 Ohm) for about 500 s after a charging-time of 100 s.

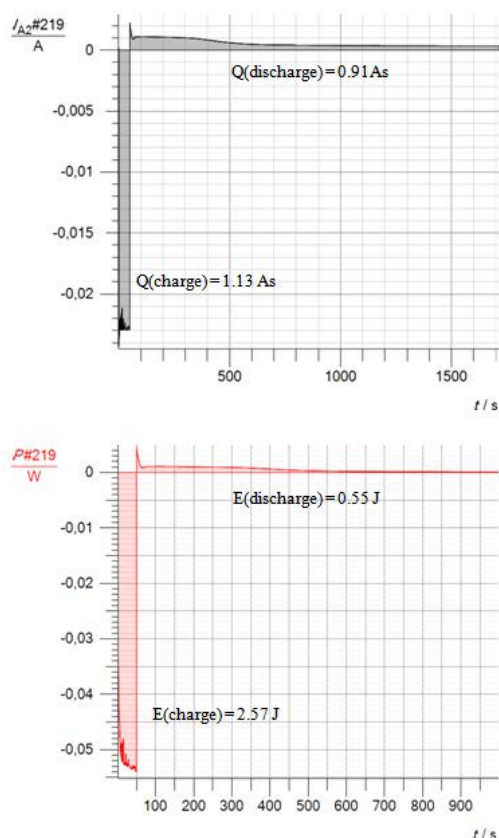


Figure 16. Top: charge for charging and for discharging. Bottom: charge energy: 2.57 J, discharge energy: 0.55 J, efficiency: 25%

As mentioned above, one can calculate the charge for charging and discharging, the energy, and the efficiency (Figure 16).

The relation between the charge for charging and discharging is about one: practically no charges are lost in the experimental test.

Of course, the efficiency of about 25% is much lower than those of commercial batteries which have a much larger surface. In addition, the winding of the electrodes and separators in commercial batteries is done automatically, and therefore the electrodes have no kinks and bends that can significantly influence both voltage and current.

4. Conclusion

The systematic investigation of the alkaline Ag-Zn and Cu-Zn batteries started more than 100 years ago. From the 1950s to the 1980s the electrode processes were examined via cyclic voltammetry followed by surface-analytical methods. Therefore, the processes are currently clarified in general.

Hence, in a didactical sense, these batteries are suitable to teach electrochemistry to

- measure, reproduce, and explain the CVs
- to observe the electrode-changes
- to charge and discharge the batteries
- to operate a motor and monitor the voltage breakdown
- to calculate the charge in the charging and discharging processes and
- to calculate the efficiency.

Therefore, we think that the investigations of alkaline Ag-Zn- and Cu-Zn-batteries are good compliments for the usually lessons contents in electrochemistry.

References

- [1] Daniel, C., Besenhardt J. O., (Eds), Handbook of Battery Materials, Vol.1 and 2, Wiley, Weinheim, 2011.
- [2] Glöckner, W., Jansen, W., Weissenhorn, R. G. (Eds.), Handbuch der experimentellen Chemie. Sekundarbereich II. Band 6: Elektrochemie, Aulis Verlag, Deubner & CoKg, Köln, 1994.
- [3] E.g. Hasselmann, M., Oetken, M., Elektrische Energie aus dem Kohlenstoffsandwich -Lithium-Ionen Akkumulatoren auf Basis redoxamphoterer Graphitinterkalationselektroden, Chemkon 3, 160-172, 2011.
- [4] Hasselmann, M., Friedrich, J., Klaus, M., Wagner, C., Moessner, B., Quarthal, D., Oetken, M., Chemie und Energie, Elektrochemischer Speichersysteme für die Zukunft, PdN- ChiS 61, 876-881, 2014.
- [5] M. Hasselmann, M. Oetken, Chemie und Energie Elektrochemische Speichersysteme für die Zukunft - Teil 2: Der Graphitminen-Akkumulator, PdN-ChiS 62, 33-43, 2013.
- [6] Aristov, N., Habekost, A., Cyclic voltammetry- A versatile electrochemical method investigating electron transfer processes, World J. Chem. Educ., 3, 115-119, 2015
- [7] Compton, B. R. G., Banks, C. E., Understanding Voltammetry, 2nd Edition, Imperial College Press, 2011.
- [8] Lorimer, J. P., Mason, T. J., Plattes, M., Walton, D. J., Passivation phenomena during sonovoltammetric studies on copper in strongly alkaline solutions, J. Electroanal. Chem., 568, 379- 390, 2004.
- [9] <https://scifinder.cas.org/scifinder/view/scifinder/scifinderExplore.jsf>
- [10] Jakes, P. J., Wong, T-L., Humphrey, T., Carlson, J.R., Cromer, D., Battery management for optimizing battery and service life, US 8244312 B2 20120814, U.S., 2012.

- [11] Stonehard, P., Portante, F. P., Potentiodynamic examination of surface processes and kinetic for the $\text{Ag}_2\text{O}/\text{AgO}/\text{OH}^-$ system, *Electrochim. Acta* 13, 1805-1814, 1968.
- [12] Speiser, B., *Elektroanalytische Methoden I: Elektrodenreaktionen und Chronoamperometrie*, *ChiuZ* 15, 21-26, 1981.
- [13] Pound, B. G., Macdonald, D. D., Tomlinson, J. W., The electrochemistry of silver in KOH at elevated temperatures - II. Cyclic voltammetry and galvanostatic charging studies, *Electrochim. Acta* 25, 563-573, 1980.
- [14] Pound, B. G., Macdonald, D. D., Tomlinson, J. W., The electrochemistry of silver in KOH at elevated temperatures - III. Potentiostatic studies, *Electrochim. Acta* 25, 1293-1296, 1980.
- [15] Lazarescu, V., Radovici, O., Vass, M., Voltametric studies on anodic oxidation of silver, *Electrochim. Acta* 30, 1407-1408, 1985.
- [16] Giles, R. D., Harrison, J. A., Potentiodynamic sweep measurement of the anodic oxidation of silver in alkaline solutions, *Electroanal. Chem. and Interfac. Electrochem.* 27, 161-163, 1970.
- [17] Popkirov, G. S., Burmeiser, M., Schindler, R. N., Electrode potential redistribution during silver oxidation and reduction in alkaline solution, *J. Electroanal. Chem.* 380, 249-254, 1995.
- [18] Droog, J. M. M., Huisman, F., Electrochemical formation and reduction of silver oxides in alkaline media, *J. Electroanal. Chem. and Interfac. Electrochem.* 115, 211-224, 1980.
- [19] McMillan, J. A., Magnetic properties and crystalline structure of AgO , *J. Inorg. Nucl. Chem.* 13, 28-31, 1960.
- [20] Servian, J. L., Buenfama, H. D., On the structure of AgO , *Inorg. Nucl. Chem. Lett.* 5, 337-338, 1969.
- [21] Yvon, K., Bezing, A., Tissot, P., Fischer, P., Structure and magnetic properties of tetragonal silver(I,III) oxide, AgO , *J. Solid State Chem.* 65, 225-230, 1986.
- [22] E.g. Hollemann, Wiberg, *Lehrbuch der Anorganischen Chemie*, 91. - 100. Auflage, Walter de Gruyter, Berlin, S. 1017, 1985.
- [23] Allen, A., The silver oxides, in: Gutmann, J. A., Friend, F., *Proceedings of the first Australian conference on Electrochemistry*, Pergamon Press, Oxford, 72-88, 1965.
- [24] Dierkse, T. P., The oxidation of the silver electrode in alkaline solutions, *J. Electrochem. Soc.* 106, 920-925, 1959.
- [25] Dierkse, T. P., The $\text{AgO} - \text{Ag}_2\text{O}$ Electrode in Alkaline Solution, *Jour. Electrochem. Soc.* 109, 173-177, 1962.
- [26] Dierkse, T. P., The cathodic behavior of AgO in alkaline solutions, *Jour. Electrochem. Soc.* 107, 859-864, 1960.
- [27] Luther, R., Pokorny, F., Über das elektrochemische Verhalten des Silbers und seiner Oxyde, *Zeitschrift für Anorganische Chemie* 57, 290-310, 1908.
- [28] https://de.wikipedia.org/wiki/Akkumulator#Energiedichte_und_Wirkungsgrad (25.8.15, 4 pm).
- [29] Schoop, P., Hat der alkalische Zink-Kupfer-Akkumulator Aussicht auf baldige praktische Verwendung im Trambetrieb?, *Zeitschrift für Elektrotechnik und Elektrochemie*, 1, 131-134, 1894.
- [30] Leckie, H. P., Anodic polarization behavior, *J. Electrochem. Soc.*, 117, 1478-1483, 1970.
- [31] Ambrose, J., Barradas, R. G., Shoesmith, D. W., Investigations of copper on aqueous alkaline solutions, *Electroanal. Chem. Interfac. Electrochem.*, 47, 47-64, 1973.
- [32] Dong, S., Xie, Y., Cheng, G., Cyclic voltammetry and spectroelectrochemical studies of copper in alkaline solution, *Electrochim. Acta*, 37, 17-22, 1992.
- [33] El Haleem, S. M., Ateya, B. G., Cyclic voltammetry of copper in sodium hydroxide, *J. Electroanal. Chem.*, 117, 309-319, 1981.
- [34] Strehblow, H.-H., Maurice, V., Marcus, P., Initial and later stages of anodic oxide formation on Cu, chemical aspects, structure and electronic properties, *Electrochim. Acta*, 46, 3755-3766, 2001.
- [35] Baricuatro, J. H., Ehlers, C. B., Cummins, K. D., Soriaga, M. P., Stickney, J. I., Structure and composition of $\text{Cu}(hkl)$ surface exposed to O_2 and emerged from alkaline solutions: Prelude to UHV-EC studies of CO_2 reduction at well-defined copper catalysts, *J. Electroanal. Chem.*, 716, 101-105, 2014.
- [36] Zhou, G., Yang, J. C., Temperature effects on the growth of oxide islands on $\text{Cu}(110)$, *Appl. surf. sci.* 222, 357-364, 2004.
- [37] Zhou, G., Yang, J. C., Temperature effect on the Cu_2O oxide morphology created by oxidation of $\text{Cu}(001)$ as investigated by in situ UHV TEM, *Appl. surf. sci.*, 210, 165-170, 2003.
- [38] Zhou, G., Yang, J. C., Initial oxidation kinetics of copper (110) film investigated by in situ UHV-TEM, *Surf. sci.*, 531, 359-367, 2003.
- [39] Beverskog, B., Puigdomenech, I., Revised Pourbaix Diagrams for Copper at 25 to 300°C, *J. Electrochem. Soc.*, 144, 3476-3483, 1997.